Effective properties of terahertz double split-ring resonators at oblique incidence

Christoph Menzel,[1,*] Ranjan Singh,[2] Carsten Rockstuhl,[1] Weili Zhang,[2] and Falk Lederer[1]

[1]*Institute of Solid State Theory and Optics, Friedrich-Schiller-Universität Jena, Max-Wien-Platz 1, Jena 07743, Germany*

[2]*School of Electrical and Computer Engineering, Oklahoma State University, Stillwater, Oklahoma 74078, USA*

[*]*Corresponding author: Christoph.Menzel@uni-jena.de*

Received July 31, 2009; revised October 20, 2009; accepted October 20, 2009; posted October 20, 2009 (Doc. ID 115062); published November 20, 2009

By combining experimental and theoretical efforts we study the optical properties of single-layer, double split-ring resonators at oblique incidences for terahertz frequencies and reveal their angular dependent effective properties. Contrary to what is usually anticipated, for incidence angles deviating from normal we do not observe any significant dispersion in the effective permeability. Effective properties are dominated instead by a strong dispersion in the effective permittivity, causing also the wavenumber in the medium to be large. The structure is shown to possess almost invariant effective properties for oblique incidences. © 2009 Optical Society of America

OCIS codes: 160.3918, 240.5420, 260.5740, 160.4760.

1. INTRODUCTION

With the ability to structure materials at the microscale and nanoscale, metamaterials (MMs) can be designed for various spectral realms ranging from the GHz down to the optical domain [1–3]. A MM is typically understood as a periodic arrangement of identical unit cells called meta-atoms. It shows an optical response that is predominantly governed by the shape of the meta-atoms and not by the materials they are made from. If the unit cells are sufficiently small, effective properties can be attributed to the MM facilitating the description of light propagation. By properly designing the meta-atoms, the optical response and thereby the optical properties can be tuned beyond those of naturally occurring materials. Probably the most fascinating property is that of negative refraction [4]. It can be achieved by combining metallic wires, which provide a negative effective permittivity, with meta-atoms showing an artificial magnetic response [5,6]. The prototypical meta-atom serving this purpose is the split-ring resonator (SRR). It was initially designed to operate in the microwave regime. In recent years the SRR concept was translated, passing the terahertz domain (THz) into the optical regime [7–9]. In particular, in the visible spectral domain the SRR concept is extended to more simple and scalable meta-atoms such as the double cutwire structure [10,11]. Besides being used to achieve negative refraction, SRRs are also used for other applications such as optical sensing [12,13].

The latter structural modification was mandatory, since the illumination direction has to be aligned to the SRR plane to observe a magnetic response from the SRR. This is difficult to achieve at optical frequencies because in most cases, detrimental for the concept, nano fabrication technologies are generally restricted to planar structures [14,15]. Consequently, in most cases the SRR properties are probed at normal incidence only. Although it was shown that the SRR resonances remain excitable in this planar configuration [16], the MM possesses only strong dispersion in the effective permittivity. No variations in the permeability when compared to vacuum is observed. It is reasonable to infer that the induced magnetic dipole moment is aligned along the optical axis. It generates, therefore, no scattered light in either the forward or the backward direction. To overcome this limitation and to probe for dispersive features in the effective permeability, it seems to be required to illuminate the structure at oblique incidence.

Although such an angular dependent spectroscopy at SRRs was accomplished [17] before, effective parameters were not assigned thus far to the structure by an appropriate retrieval procedure. In most cases this retrieval is performed by inverting the Fresnel coefficients for an equivalent homogeneous slab with unknown permittivity and permeability [18]. Since it is usually done at normal incidence only, the question has remained open as to whether it is possible to observe a noticeable dispersion in the effective permeability at oblique incidences.

To resolve this issue, here we investigate the spectral response and, most notably, the effective properties of double split-ring resonators (DSRRs) by THz-time domain spectroscopy at oblique incidences [19,20]. The DSRR was chosen since it is known to exhibit an artificial magnetic response, which is an important ingredient for negative refraction [21]. In general, the DSRR is a complicated optical structure, showing strong polarization changes for various incidence planes and polarization directions. These changes are induced by the bianisotropy of the structure. This magneto-electric coupling has to be taken into account to properly describe the optical response [22,23]. It complicates, in general, the retrieval. Nonetheless, for certain combinations of polarization states and planes of incidence, the structure leaves the state of po-

larization invariant. In these cases the retrieval of effective parameters by inverting the Fresnel coefficients, extended to the scenario of oblique incidence as detailed in [24], can be applied.

2. EXPERIMENTAL RESULTS

The considered geometry is shown in Fig. 1. The unit cells comprising the DSRR are arranged on a square lattice with $P_x = P_y = 50\ \mu$m. By restricting ourselves to cases where the incidence plane is aligned with a crystallographic axis [(implying that either $k_x = 0$ or $k_y = 0$) four different combinations of incidence plane and a polarization state are possible where the polarization is maintained for two cases only, shown in Fig. 1(a)]. In what follows, we restrict ourselves to these cases and designate them as TE and TM cases. The nomenclature reflects whether the incident electric or the magnetic field component is normal to the plane of incidence, respectively. The DSRRs are made from aluminum and fabricated by photolithography. They are deposited on a silicon substrate with $\epsilon_{\mathrm{Sub}} = 11.68$. The thickness of the substrate was 640 μm. Note that the single DSRR layer has a thickness of only 200 nm [25]. The spectra were measured by illuminating the sample with a few-cycle THz pulse, and the time-dependent transmission was detected. By Fourier transforming the time trace, the spectral response is obtained. All transmission spectra were normalized by that of the silicon substrate only at the same angle of incidence. This experimental procedure was fully reproduced in the post-processing of the numerical data to allow for a comparison. The raw numerical data were obtained with the Fourier modal method [26]. It is a rigorous numerical technique to calculate the diffraction response from a bi-periodic structure. In this simulation we took fully into account the nominal fabrication geometry and the spectral dependent material parameters. Furthermore, we assumed that the substrate is infinitely extended. It reflects the experimental procedure where the time trace was truncated prior to the arrival of multiple reflections from the backside of the substrate at the detector. Note that this truncation does not affect the spectra, as the lifetime of all excitable resonances is much smaller than the arrival time of the back-reflected pulse. The time-domain signal at the moment of truncation is in the order of the background noise level. Therefore it is possible to increase the frequency resolution by a factor of 8 by zero-padding the time-domain signal. This normalized numerical and experimental data for the complex transmitted amplitude are shown in Fig. 2.

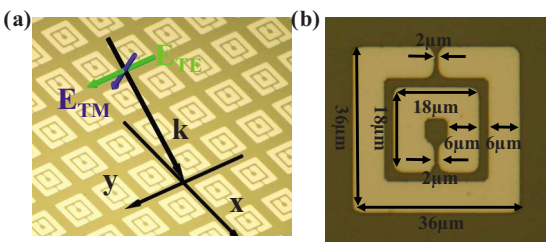

Fig. 1. (Color online) Sketch of the geometry. (a) Periodic arrangement of the DSRR together with the relevant propagation directions and polarization states. (b) Single DSRR with relevant dimensions.

The spectra, shown in Fig. 2, correspond to several angles of incidence for TE and TM polarization. Good agreement between theory and measurement is noted. Clearly, the spectral response of the structure depends strongly on the polarization, since different eigenmodes of the DSRR were excited for different polarizations [27–30].

For TE polarization, the electric field is parallel to the DSRR base, hence odd eigenmodes of the DSRR can only be excited. The lowest-order eigenmode excited at the smallest frequency (0.5 THz) is the first-order mode. It is usually denoted as the LC mode [6]. The notation of the resonance as the first-order mode derives from the number of nodes in the amplitude of the electric field component normal to the surface. The mode is characterized by a ring current with no nodes flowing along the wires. It results in a magnetic dipole moment via Lenz's law. At normal incidence the magnetic dipole moment is aligned with the illumination direction. Since the meta-atoms are periodically arranged on a subwavelength scale, the radiation annihilates due to destructive interference except in the forward (backward) direction. But since the induced magnetic dipole moment is not radiating in the forward (backward) direction, no noticeable magnetic dispersion will be observed for normal incidence. This magnetic dipole moment is usually assumed to be radiative as soon as the angle of incidence deviates from the normal. It may be anticipated that this affects the effective permeability.

For TE polarization it can be furthermore seen that the third-order eigenmode is excited at 1.6 THz resulting in a

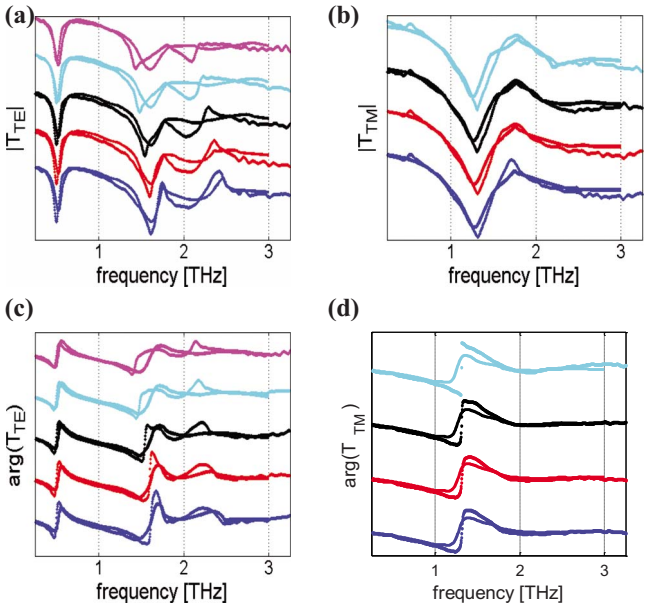

Fig. 2. (Color online) Complex amplitude for the simulated (solid curves) and the measured transmission (dotted lines). The modulus ((a) TE polarization and (b) TM polarization) and the phases ((c) TE polarization and (d) TM polarization) are shown. The different lines correspond to different angles of incidence: blue, 0 deg; red, 15; black, 30; cyan, 45; magenta, 60. An arbitrary offset was added to each data to separate them in the figure. The frequency resolution of the experimental data is 3.6 GHz and 11.5 GHz for the numerical data.

nonvanishing averaged current oscillating in the ring. Therefore, it is similarly expected that this mode might cause a dispersive effective permeability at oblique incidence.

For TM polarization the electric field is parallel to the DSRR side arms. Since the exciting field is identical in both arms, i.e., for symmetry reasons, only even-order eigenmodes are excitable. The first even-order eigenmode is excited at 1.3 THz. This resonance is usually called the plasmon resonance of the SRR, since it is associated with currents oscillating in-phase in both side arms of the SRR. It mimics the response of an electric dipole antenna. Consequently, it will affect the effective permittivity. It is not anticipated that this behavior is modified at oblique incidence.

3. EFFECTIVE PROPERTIES

Since experimental results for the complex amplitudes are only at hand for transmission, we rely in the subsequent retrieval on the numerically obtained complex transmission and reflection coefficients. By using the algorithm described in [24], the effective propagation constant, the effective permittivity and the effective permeability are retrieved for all angles of incidence and both polarizations. The results for their real and imaginary parts are shown in Fig. 3. By considering at first TE polarization, we notice that the absolute values of the permittivity, as well as the quality factors of the resonances, are very large. The induced dispersion is strongest for the lowest-order resonance. The tremendous magnitude of the dispersion is attributed to the actual small thickness of the MM ($h=200$ nm) that was retained in the retrieval. The MM acts as a thin sheet and not as a bulk material. Therefore the effective parameters, as shown in Fig. 3, have to be understood as the angle- and wavelength-dependent optical properties of an equivalent homogenous thin film that causes the same reflection and transmission coefficients as the patterned nanostructure. They should be therefore termed as wave parameters.

Furthermore, we do not observe any dispersion in the effective permeability, implying that a potential magnetic response cannot be probed at oblique incidence for the chosen polarization, although the incident magnetic field has a component normal to the DSRR plane. Since the permeability is only slightly deviating from unity, the effective refractive index of the DSRR layer is quite large too and reaches values of about 50, as can be seen in Fig. 4. Here we show the real and the imaginary parts of the normalized propagation constant k_z/k_0. For normal incidence, k_z/k_0 is identical to the effective refractive index n_{eff}. Since these values are almost constant for all angles of incidence, the phase advance for propagation through the thin layer is independent on the angle. This is an important and peculiar property of this class of MM. This also explains why dispersion in the effective permeability and permittivity is not observed. The wave vector in the pertinent THz MM is much larger when compared to the outer region because of the large effective index. Thus one may conclude that for oblique incidences the transverse wave vector component is negligible when compared to its modulus. Therefore, although illuminated at oblique incidence, the effective properties, probed by plane waves propagating inside the medium, are only slightly deviating from those for normal incidence.

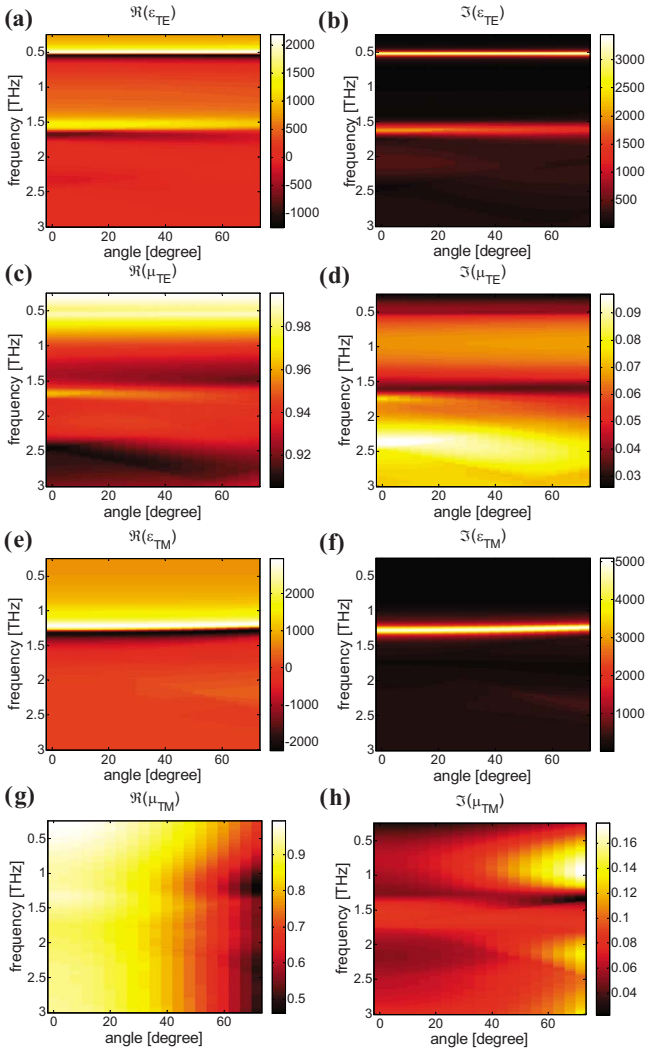

Fig. 3. (Color online) Real and imaginary parts of the effective permittivity and permeability as a function of the frequency and the angle of incidence. (a)–(d) TE polarization, (e)–(h) TM polarization. The effective parameters were retrieved from the numerically obtained complex reflection and transmission coefficients. Note that the Lorentzian resonances in the effective permittivity have very large quality factors, whereas the effective permeability is almost unaffected for all angles of incidence.

For TM polarization, the situation is similar. Whereas the effective permittivity attains large values resulting in a large effective refractive index, the effective permeability remains close to unity. The spectral response is again only slightly modified by varying the angle of incidence as outlined above.

4. CONCLUSIONS

In conclusion, we revealed the angular dependent effective properties that can be attributed to a THz MM made from DSRRs. The work comprises experimental results corroborated with numerical simulations. It was shown that the effective properties are almost independent of the angle of incidence. Strong dispersion was observed in

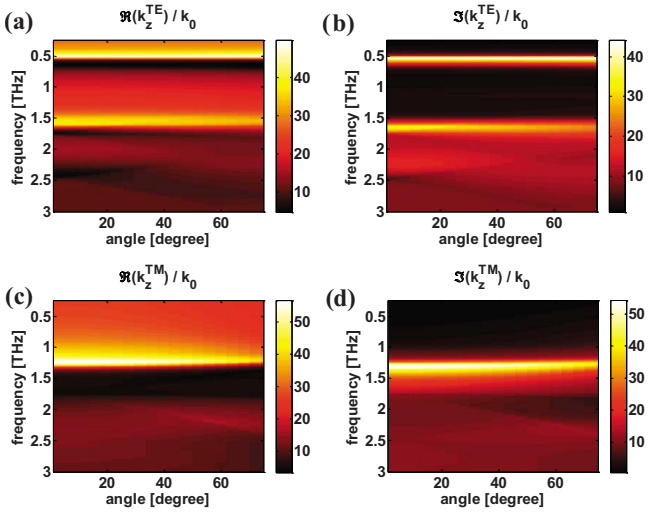

Fig. 4. (Color online) Real and imaginary parts of the propagation constant k_z as a function of the frequency and the angle of incidence as retrieved from the numerically obtained complex reflection and transmission coefficients. (a), (b) TE polarization, (c), (d) TM polarization.

the effective permittivity, whereas it was not noticed in the effective permeability. This counterintuitive behavior may potentially be attributed to the large effective index of the medium. It prohibits the excitation of nonparaxial beam components in the medium, rendering it possible to probe only for properties close to normal incidence. Therefore, it remains open to perform comparable measurements at optical frequencies where the induced dispersion in the effective properties is less severe and where it should be easier to accomplish an excitation of plane waves with propagation directions inside the medium that strongly deviate from the optical axis.

ACKNOWLEDGMENTS

This work was partially supported by the U.S. National Science Foundation (NSF), the German Federal Ministry of Education and Research (Metamat), and the Thuringian State Government (MeMa). Some computations utilized the IBM p690 cluster JUMP of the Forschungszentrum Jülich, Germany. The authors thank S. Fahr for support in figure preparation.

REFERENCES

1. C. M. Soukoulis, S. Linden, and M. Wegener, "Physics: negative refractive index at optical wavelengths," Science **315**, 47–49 (2007).
2. V. M. Shalaev, "Optical negative-index metamaterials," Nature Photon. **1**, 41–48 (2007).
3. R. A. Shelby, D. R. Smith, and S. Schultz, "Experimental verification of a negative index of refraction," Science **292**, 77–79 (2001).
4. J. B. Pendry, "Negative refraction makes a perfect lens," Phys. Rev. Lett. **85**, 3966–3969 (2000).
5. T. J. Yen, W. J. Padilla, N. Fang, D. C. Vier, D. R. Smith, J. B. Pendry, D. N. Basov and X. Zhang, "Terahertz magnetic response from artificial materials," Science **303**, 1494–1496 (2004).
6. C. Enkrich, M. Wegener, S. Linden, S. Burger, L. Zschiedrich, F. Schmidt, J. F. Zhou, Th. Koschny, and C. M. Soukoulis, "Magnetic metamaterials at telecommunication and visible frequencies," Phys. Rev. Lett. **95**, 203901 (2005).
7. B. Kanté, A. de Lustrac, J.-M. Lourtioz, and F. Gadot, "Engineering resonances in infrared metamaterials," Opt. Express **16**, 6774–6784 (2008).
8. J. Zhou, T. Koschny, and C. M. Soukoulis, "Magnetic and electric excitations in split ring resonators," Opt. Express **15**, 17881–17890 (2007).
9. A. W. Clark, A. K. Sheridan, A. Glidle, D. R. S. Cumming, and J. M. Cooper, "Tuneable visible resonances in crescent shaped nano-split-ring resonators," Appl. Phys. Lett. **91**, 093109 (2007).
10. G. Dolling, C. Enkrich, M. Wegener, J. F. Zhou, C. M. Soukoulis and S. Linden, "Cut-wire pairs and plate pairs as magnetic atoms for optical metamaterials," Opt. Lett. **30**, 3198–3200 (2005).
11. V. M. Shalaev, W. Cai, U. K. Chettiar, H.-K. Yuan, A. K. Sarychev, V. P. Drachev, and A. V. Kildishev, "Negative index of refraction in optical metamaterials," Opt. Lett. **30**, 3356–3358 (2005).
12. J. F. O'Hara, R. Singh, I. Brener, E. Smirnova, J. Han, A. J. Taylor, and W. Zhang, "Thin film sensing with planar terahertz metamaterials: sensitivity and limitations," Opt. Express **16**, 1786–1795 (2008).
13. B. Lahiri, A. Z. Khokhar, R. M. De La Rue, S. G. McMeekin, and N. P. Johnson, "Asymmetric split ring resonators for optical sensing of organic materials," Opt. Express **17**, 1107–1115 (2009).
14. A. Boltasseva and V. M. Shalaev, "Fabrication of optical negative-index metamaterials: Recent advances and outlook," Metamaterials **1**, 1–17 (2008).
15. M. C. Gwinner, E. Koroknay, L. Fu, P. Patoka, W. Kandulski, M. Giersig, and H. Giessen, "Periodic large-area metallic split-ring resonator metamaterial fabrication based on shadow nanosphere lithography," Small **5**, 400–406 (2009).
16. C. Rockstuhl, T. Zentgraf, E. Pshenay-Severin, J. Petschulat, A. Chipouline, J. Kuhl, T. Pertsch, H. Giessen, and F. Lederer, "The origin of magnetic polarizability in metamaterials at optical frequencies–an electrodynamic approach," Opt. Express **15**, 8871–8883 (2007).
17. T. Driscoll, D. N. Basov, W. J. Padilla, J. J. Mock, and D. R. Smith, "Electromagnetic characterization of planar metamaterials by oblique angle spectroscopic measurements," Phys. Rev. B **75**, 115114 (2007).
18. D. R. Smith, S. Schultz, P. Markoš, and C. M. Soukoulis, "Determination of effective permittivity and permeability of metamaterials from reflection and transmission coefficients," Phys. Rev. B **65**, 195104 (2002).
19. D. Grischkowsky, S. Keiding, M. van Exter, and Ch. Fattinger, "Far-infrared time-domain spectroscopy with terahertz beams of dielectrics and semiconductors," J. Opt. Soc. Am. B **7**, 2006–2015 (1990).
20. R. Singh, E. Smirnova, A. J. Taylor, J. F. O'Hara, and W. Zhang, "Optically thin terahertz metamaterials," Opt. Express **16**, 6537–6543 (2008).
21. J. B. Pendry, A. J. Holden, D. J. Robbins, and W. J. Stewart, "Magnetism from conductors and enhanced nonlinear phenomena," IEEE Trans. Microwave Theory Tech. **47**, 2075–2084 (1999).
22. X. Chen, B.-I. Wu, J. A. Kong, and T. M. Grzegorczyk, "Retrieval of the effective constitutive parameters of bianisotropic metamaterials," Phys. Rev. E **71**, 046610 (2005).
23. Z. Li, K. Aydin, and E. Ozbay, "Determination of the effective constitutive parameters of bianisotropic metamaterials from reflection and transmission coefficients," Phys. Rev. E **79**, 026610 (2009).
24. C. Menzel, C. Rockstuhl, T. Paul, T. Pertsch, and F. Lederer, "Retrieving effective parameters for metamaterials at oblique incidence," Phys. Rev. B **77**, 195328 (2008).
25. A. K. Azad, J. Dai, and W. Zhang, "Transmission properties of terahertz pulses through subwavelength double split ring resonators," Opt. Lett. **31**, 634–636 (2006).
26. L. Li, "New formulation of the Fourier modal method for crossed surface-relief gratings," J. Opt. Soc. Am. A **14**,

2758–2767 (1997).
27. N. Katsarakis, T. Koschny, M. Kafesaki, E. N. Economou, and C. M. Soukoulis, "Electric coupling to the magnetic resonance of split ring resonators," Appl. Phys. Lett. **84**, 2943–2945 (2004).
28. C. Rockstuhl, T. Zentgraf, T. P. Meyrath, H. Giessen, and F. Lederer, "Resonances in complementary metamaterials and nanoapertures," Opt. Express **16**, 2080–2090 (2008).
29. F. J. Rodriguez-Fortuno, C. Garcia-Meca, R. Ortuno, J. Marti, and A. Martinez, "Role of surface plasmon polaritons on optical transmission through double layer metallic hole arrays," Phys. Rev. B **79**, 075103 (2009).
30. T. Zentgraf, J. Dorfmüller, C. Rockstuhl, C. Etrich, R. Vogelgesang, K. Kern, T. Pertsch, F. Lederer, and H. Giessen, "Amplitude- and phase-resolved optical near fields of split-ring-resonator-based metamaterials," Opt. Lett. **33**, 848–850 (2008).